PRAMANA
— journal of
physics

Vol. 44, No. 1,
January 1995
pp. 55–66

Dynamics of a collisional ion sheath

S MUKHERJEE and P I JOHN
Institute for Plasma Research, Bhat, Gandhinagar 382424, India

MS received 23 September 1994

Abstract. Experiments on collisional ion sheaths are carried out by applying a pulsed negative bias on a disc electrode immersed in a collisional plasma. The pulse is characterized by a linear rise, followed by a constant voltage phase and then exponential decay. The measured currents to the electrode are compared to predictions from a dynamic collisional ion sheath model which is developed from the basic two fluid equations. The parameter determining the degree of collisionality is also defined. The agreement between the two in the rising and the flat top phases of the pulse is found to be good. Some residual discrepancies as well as the disagreement in the decay phase are discussed.

Keywords. Collisional ion sheaths; constant mean free path; dynamic collisional sheath thickness; secondary electron emission.

PACS No. 52·40

1. Introduction

The dynamics of collisional ion sheaths is receiving increasing attention these days. Several recent experiments [1–3] have demonstrated that more analysis of the collisional sheaths are required. The essential feature that makes the study of collisional dynamic ion sheaths interesting is that the ions in the sheath cannot get the entire energy from the field. A significant portion of the energy is lost by collisions with the neutrals. The validity of using a quasistatic Child's law when the sheath is in evolution is therefore not justified and there exists a need to derive a proper dynamic collisional law.

On the other hand, the dynamics of collisionless sheaths has been extensively studied, partly due to its importance in many applications [4–10]. For example, in plasma immersion ion implantation (PIII) [4], which is a relatively new and non-line-of-sight technique for surface modifications of materials, the collisionless sheath plays a crucial role in accelerating the ions and getting them implanted. Some features are common to both collisional and collisionless sheaths [10, 11]. In both the cases the current demanded by the electrode is given by sheath expansion. This exposes more ions to the potential and permits them to respond to it.

At lower operating pressures (10^{-4} torr) [4–10] the mean free path of ion neutral collisions is generally larger than the typical sheath dimensions making the sheath essentially collisionless. Among the ion neutral collisions that take place in the sheath, charge exchange collisions have the highest cross section. Also for a large energy range their cross sections remain fairly constant [1–3, 11]. Collisional sheath experiments are carried out at higher pressures ($\sim$ 50 m torr) which makes the mean free path of ion neutral collisions smaller than the sheath dimensions. Hence an ion

may lose a significant portion of its energy by collisions, before reaching the electrode.

In this paper we report on experiments, carried out on a disc electrode immersed in a collisional plasma, and to which a negative pulse is applied. The negative pulse is characterized by a linear rise time, followed by a flat top phase and an exponential decay. The current collected by the electrode during the pulse duration is measured. The measured currents are compared to the prediction from a theoretical model. The model is developed from the fluid equations with the inclusion of appropriate collisional terms to permit the study of collisional sheaths. The model is found to yield generally good results in the rising and the flat top phase of the pulse. The small residual discrepancies as well as the disagreement during the decay region are discussed in terms of the shortcomings of the model.

2. Experimental set up

The experiments are performed (figure 1) in a cylindrical chamber made of stainless steel of diameter 50 cm and length 120 cm. The chamber is pumped down to $1{\cdot}0 \times 10^{-5}$ torr and is brought to the operating pressure by filling with argon. Two sets of filaments at the ends of the chamber are heated using two separate power supplies. Thermoionic electrons emitted from the filaments are accelerated into the chamber, where they undergo collisions with argon atoms producing a plasma. The filament current and the discharge current can be adjusted to get a uniform plasma in the experimental region. In the pressure range (1–100 mtorr) in which the experiments are carried out, $T_e \approx 3$ eV and n_i can be varied between $1{\cdot}0$–$10{\cdot}0 \times 10^8$ per cc. The ions are assumed to be at room temperature.

In the center of the cylindrical chamber a stainless steel disc electrode of diameter 20 cm is kept with its surface normal to the axis of the chamber. Negative pulses of magnitude 400 V and pulse duration of 12 μs are applied on the disc. The rise time of the pulse is about $1{\cdot}4\,\mu$s and is linear, with a flat top phase of $3{\cdot}6\,\mu$s and an exponential decay with time constant of $2{\cdot}52\,\mu$s (figure 2). The pulse satisfies the criterion that the applied bias is much larger than T_e and each section of the pulse is larger than the ion plasma period. The pulses are produced [12] by discharging a previously charged LC network across the characteristic resistance of the LC line. The drop across the resistance is connected to the disc electrode through a capacitor (figure 3). This arrangement keeps the electrode at the floating potential in the absence of the pulse. The current collected by the electrode is measured by a Pearson current transformer and the current is noted during the entire pulse period. The capacitor also prevents any dc current to flow through the current transformer.

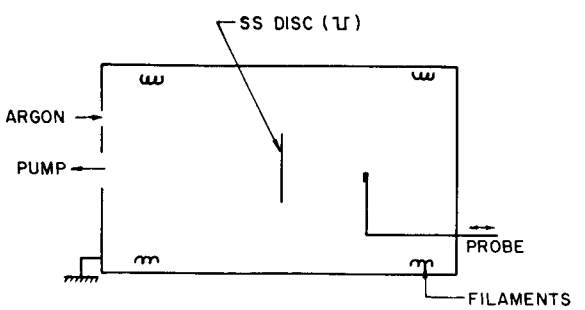

Figure 1. Experimental set up.

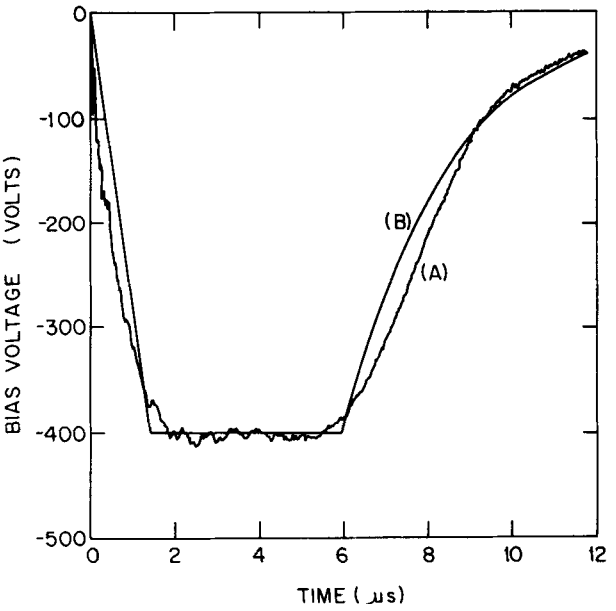

Figure 2. Pulse shapes used in: [A] Experiment [B] Calculation (eq. 15). $\phi_0 = 400\,\text{V}$ and $\tau = 2{\cdot}52\,\mu\text{s}$.

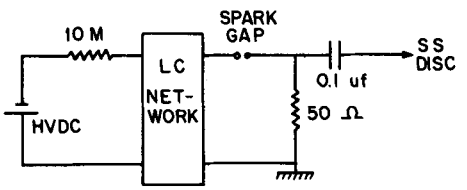

Figure 3. Schematic diagram of the pulse forming circuit.

The experimental current is shown in figure 5 (trace A) and figure 6 (trace A). Both the traces indicate identical overall behaviour. During the rise time of the applied bias the current increases. In the flat top phase the current starts decreasing from its value at the end of the rise time. During the decay phase of the pulse, the current further decreases and becomes negative and then goes to zero at the end of the pulse.

3. Collisional sheath model and its application

For a more quantitative understanding of the experimental results a theoretical model is developed. The model is based on the fluid treatment of the ions and the electrons. We begin with the static model and then extend it to include time evolution so that the dynamics of the ion sheaths can be understood.

3.1 *Derivation of the static collisional sheath model*

The derivation of the collisional sheath model is made by using the fluid equations for the ions and electrons. The electrons are assumed to satisfy a Boltzman distribution. This assumption is valid when the time scales of interest are much longer than the

electron plasma time scales. Hence the electron density can be written as,

$$n_e = n_0 \exp(e\phi/kT_e) \tag{1}$$

where e is the electronic charge, k is the Boltzman's constant and T_e denotes the electron temperature. As shown in [3] the dominant collisions in the sheath are ion neutral collisions, specially charge exchange. These collisions are source free, hence conserving ion flux and are also characterized by the property of constant mean free path. We will be restricting ourselves to one dimensional planar calculations. The time stationary ion continuity and momentum equation is

$$\partial_x(n_i v_i) = 0 \tag{2}$$

$$M_i v_i \partial_x v_i = -e\partial_x \phi - M_i n_n \sigma v_i^2 \tag{3}$$

where M_i, v_i, n_i are the ion mass, velocity and density respectively. σ and ϕ are the cross section and potential respectively. Poisson's equation completes the set of model equations, and the self consistent potential in the collisional sheath is obtained

$$\varepsilon_0 \partial_x^2 \phi = -e(n_i - n_e). \tag{4}$$

We make the equations dimensionless by using the following transformations. [$\eta = -e\phi/kT_e, \xi = x/\lambda_d, u = v_i/c_s$ and $\alpha = \lambda_d n_n \sigma = \lambda_d/\lambda_{mfp}$]. The dimensionless set of equations are

$$\eta' = u u' + \alpha u^2 \tag{5}$$

$$\eta'' = u_0/u - \exp(-\eta). \tag{6}$$

The boundary conditions at the sheat plasma interface are at $\xi = 0, u = u_0, \eta = 0$ and $\eta' = 0$ and at the electrode $\xi = d, \eta = \eta_w$. Equations (5) and (6) have been used before [13]. These nonlinear equations are difficult to solve analytically except in some simpler limits. However it is straightforward to solve them numerically. The numerical

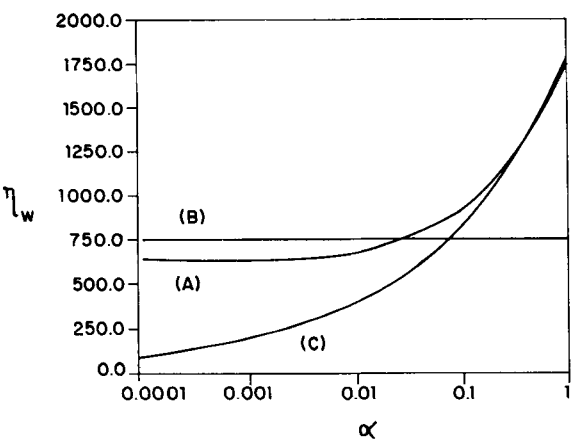

Figure 4. Dependence of η_w (dimensionless wall potential) on α (ratio of debye length to the charge exchange mean free path) for [A] exact equations (eqs 5 and 6) [B] collisionless (eqs 7 and 8) and [C] collisional (eqs 10 and 11). The sheath thickness $d = 100$ debye lengths.

solutions of (5) and (6) are carried out by keeping the sheath thickness fixed but by changing α. Each value of α gives a value of the dimensional electrode potential (η_w) such that a $\xi = 0$, $\eta = 0$. Trace (A) of figure 4 represents the results obtained from this exercise. For low values of α, η_w is independent of α and for $\alpha > 0{\cdot}01$, η_w increases with α. This essentially shows that for the same sheath thickness a collisional sheath can handle more potential difference. Hence the electric fields are stronger in a collisional sheath.

To get the Child's law [13–15], which describes the collisionless sheath, α is set equal to zero and $\eta \gg 1$ limit is taken. The second limit allows us to neglect the contribution of the electrons in determining the potential profile of the sheath. Hence,

$$\eta' = u\,u' \tag{7}$$

$$\eta'' = u_0/u. \tag{8}$$

Equations (7) and (8) are exactly solvable and gives the dimensionless version of Child's law,

$$\eta \propto \xi^{4/3} \tag{9}$$

By using (9), the value of η_w is obtained, such that at $\xi = 0$, $\eta = 0$, satisfying the boundary conditions. This is shown in trace (B) of figure 4. The η_w obtained from the (7) and (8) are independent of α and for small values of α traces (A) and (B) nearly match. Hence for a collisionless ion sheath and for high electrode bias Child's law is a satisfactory description for the sheath.

As α denotes the degree of collisionality hence for a collision dominated sheath the term containing α will have more contribution in the momentum equation (eq. 5). The limits on α are presented later in this section where this argument holds good. Hence to get the collision dominated ion sheath the term uu' is dropped in (5). The limit $\eta \gg 1$ is also taken and hence the contribution of the electrons is neglected. The equations thus obtained are

$$\eta' = \alpha u^2 \tag{10}$$

$$\eta'' = u_0/u. \tag{11}$$

Equations (10) and (11) are exactly solvable and by using the above boundary conditions the solution is

$$\eta \propto \xi^{5/3}. \tag{12}$$

Again η_w is obtained for various α using (12), such that at $\xi = 0$, $\eta = 0$. This is shown in trace (C) of figure 4. As expected η_w has a strong dependence on α and for α ranging between 0·2 to 1·0 the numerical solutions of (5) and (6) and (12) match. Hence (9) and (10) are a good description for the entire sheath properties and can be used in place of the exact eqs (5) and (6) provided α lies between 0·2 and 1·0 and $\eta \gg 1{\cdot}0$. The limits also indicate the degree of collisionality required to define an ion sheath as collisional. Equation (12) when expressed in non dimensional parameters appears to be

$$J = A\phi^{3/2}/x^{5/2} \tag{13}$$

where J is the current density and $A = \varepsilon_0(2e\lambda_i/M_i)^{1/2}\,(250/243)^{1/2}$.

Liberman [11] has proposed a collisional sheath model without specifying the degree of collisionality required for it to be valid. Though the dependences of J on ϕ and x are same in his model and our model but there is a difference between the constants by $(2/\pi)^{1/2}$. There [11] the mean ion velocity was obtained by carrying out a time averaging of the ion velocity over the distribution of mean free paths. This averaging was done because the ion motion was governed by the transport laws. In the present model the derivation starts with the fluid equations and the directed motion of ions in the sheath is a consequence of the electric field of the sheath.

3.2 *Derivation of dynamic collisional sheath thickness and the current*

To get the dynamic collisional ion sheath model eq. (13) is used in the quasistatic approximation. This is valid, provided certain assumptions that are made holds good. The assumptions are,

(a) the electron motion is inertialess and hence electrons respond instantaneously to the potential and are driven away
(b) the current required by the bias applied on the electrode at each instant of time is given by the penetration of the sheath plasma interface deeper in the plasma. This exposes more ions to respond to the potential
(c) the transit time of ions in the sheath is faster than the rate of sheath expansion
(d) the pulse time periods are larger than the ion plasma response time scales
(e) the ion motion in the sheath is collisional, with charge exchange being the dominant collision mechanism and hence the collision is characterized by the property of constant mean free path
(f) the quasistatic sheath expands with the sheath plasma interface having the same area as the electrode and also remains parallel to it at all times of evolution.

These assumptions are generally made in dealing with dynamic collisional plasma sheaths [1–3, 11, 16]. We do not put any restriction on the ion density inside the sheath as done by Vahedi *et al* [16]. In their collisional sheath model they have assumed that ion density remains constant inside the sheath which gives a parabolic potential profile inside the sheath. As indicated in (9) and (12), which describe the collisionless and the collisional sheaths, the potential profiles are not parabolic.

On the application of the bias the sheath edge moves with a speed $(\mathrm{d}x/\mathrm{d}t)$ giving a current $= en(\mathrm{d}x/\mathrm{d}t)$. The above assumptions permit us to write,

$$J = A\phi^{3/2}/x^{5/2} = en(\mathrm{d}x/\mathrm{d}t). \tag{14}$$

If the dependence of ϕ on time is known then (14) can be integrated to find out the properties of the dynamic sheath. As the interest is in estimating the current collected in the experiment, $\phi(t)$ should be the experimental pulse (figure 2). The properties of the pulse can be summarized as,

$$\frac{\phi}{\phi_0} = \begin{cases} t/t_r & 0 < t < t_r \\ 1 & t_r < t < t_r + t_p \\ \exp[(-t + t_r + t_p)/\tau] & t_r + t_p < t < t_r + t_p + t_f \end{cases} \tag{15}$$

where t_r, t_p and t_f denotes the rise time, flat top and fall time respectively. τ denotes the time constant during the falling part of the pulse. The current density can be calculated in each phase of the pulse.

3.2.1. For $0 < t < t_r$, $\dfrac{\phi}{\phi_0} = t/t_r$ hence (14) can be integrated with the boundary condition at $t = 0$, $x = 10\lambda_d$. As the electrode is initially floating (figure 3) it is justified in making this boundary condition. Hence,

$$x = [(7A/5en)(\phi_0/t_r)^{3/2} t^{5/2} + (10\lambda_d)^{7/2}]^{2/7}. \tag{16}$$

Equation (16) when substituted in (14) gives

$$J = \frac{A(\phi_0/t_r)^{3/2} t^{3/2}}{[(10\lambda_d)^{7/2} + (7A/5en)(\phi_0/t_r)^{3/2} t^{5/2}]^{5/7}} \tag{17}$$

and

$$x(t_r) = [(7A/5en)(\phi_0)^{3/2} t_r + (10\lambda_d)^{7/2}]^{2/7}. \tag{18}$$

Equation (17) indicates that in an expanding collisional plasma sheath at initial times the current density increases as $t^{3/2}$ whereas at later times it falls as $t^{4/7}$ though the bias applied can still increase linearly at time.

3.2.2. As $\phi/\phi_0 = 1$ for $t_r < t < t_r + t_p$ integration of (14) with the boundary condition at $t = t_r$, $x = x(t_r)$ (given by (18))

$$x = [(7A/2en)(\phi_0)^{3/2}(t - 3t_r/5) + (10\lambda_d)^{7/2}]^{2/7}. \tag{19}$$

The expression for J is,

$$J = \frac{A(\phi_0)^{3/2}}{[(10\lambda_d)^{7/2} + (7A/2en)(\phi_0)^{3/2}(t - 3t_r/5)]^{5/7}} \tag{20}$$

and

$$x(t_r + t_p) = [(7A/2en)(\phi_0)^{3/2}(t_p + 2t_r/5) + (10\lambda_d)^{7/2}]^{2/7}. \tag{21}$$

Though the bias does not change with time during this phase of the pulse the current density indicated by (20) goes on decreasing starting from its value given by $J(t_r)$.

3.2.3. In the third phase $\phi/\phi_0 = \exp[(-t + t_r + t_p)/\tau]$ for $t_r + t_p < t < t_r + t_p + t_f$ integration of (14) can be carried out with the boundary condition, at $t = t_r + t_p$, $x = x(t_r + t_p)$ (given by (21))

$$x = \left[(7A/en)(\phi_0)^{3/2}\left\{\frac{\tau}{3} + \frac{t_p}{2} + \frac{t_r}{3} - \frac{\tau}{3}\left(\exp\left(\frac{-t + t_r + t_p}{\tau}\right)\right)^{3/2}\right\} + (10\lambda_d)^{7/2}\right]^{2/7}. \tag{22}$$

The expression for J is,

$$J = \frac{A(\phi_0)^{3/2}\left(\exp\left(\dfrac{-t + t_r + t_p}{\tau}\right)\right)^{3/2}}{\left[(10\lambda_d)^{7/2} + (7A/en)(\phi_0)^{3/2}\left\{\dfrac{\tau}{3} + \dfrac{t_p}{2} + \dfrac{t_r}{3} - \dfrac{\tau}{3}\left(\exp\left(\dfrac{-t + t_r + t_p}{\tau}\right)\right)^{3/2}\right\}\right]^{5/7}} \tag{23}$$

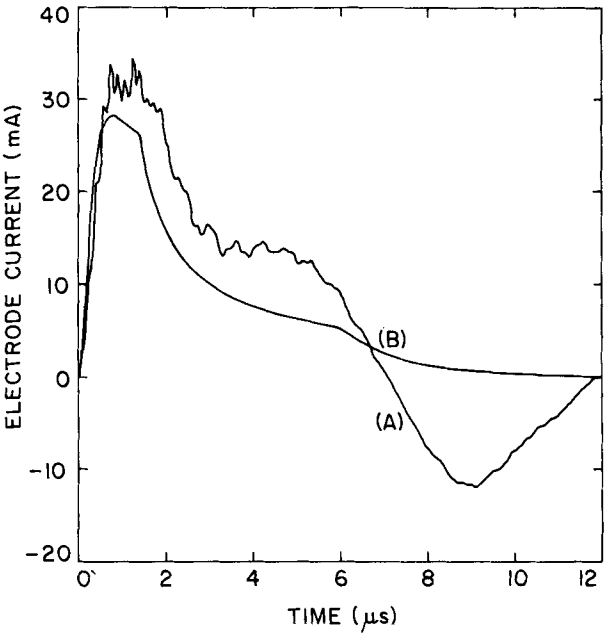

Figure 5. Comparison of the experimental [A] and the model current [B]. $n_i = 4{\cdot}04 \times 10^8\,cc^{-1}$ and $\alpha = 0{\cdot}21$.

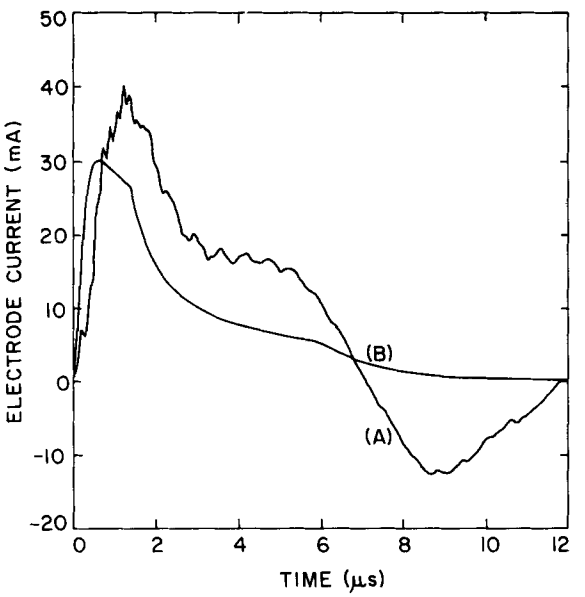

Figure 6. Comparison of the experimental [A] and the model current [B]. $n_i = 8{\cdot}1 \times 10^8\,cc^{-1}$ and $\alpha = 0{\cdot}35$.

The current further reduces starting from its value at $J(t_p)$ and goes to zero at the end of the pulse.

Thus the expressions for current density and the sheath thickness at each instant of time is known. The calculated current density (eqs 17, 20, 23) is multiplied by the area of the electrode and compared with the measured current obtained from the

experiment. The currents predicted by the model are shown in figure (5) (trace B) and figure (6) (trace B).

4. Results and discussion

The experimental conditions ensure that the plasma and the sheath is highly collisional ($0{\cdot}2 < \alpha < 1{\cdot}0$) so that comparisons can be made between the experiment and the model. In both the figures (5) and (6), during the rising part (0 to $1{\cdot}4\,\mu$s) and in the flat top phase ($1{\cdot}4$ to $6{\cdot}0\,\mu$s) of the applied pulse the agreement is good and the model indicates the general trend of the experimental current. In the falling part of the pulse ($6{\cdot}0$ to $12{\cdot}0\,\mu$s) the experimental current becomes negative and the agreement with the model is also not satisfactory. The discrepancies during each of these phases of the applied voltage pulse are discussed below.

During the rise time and the flat top phase of the pulse, the current predicted by the model is less than the measured value. It is assumed in the model that the sheath plasma interface always expands having the same area as the disc electrode. This allows us to multiply the current densities obtained from eqs. (17), (20), (23) by the electrode area to get the total current. Experiments done by Malik *et al* [6] has proved that the sheath produced by a planar electrode expands in all directions and is not confined to expand only in one direction. Expansion in other directions will expose more ions to respond to the electrode potential and hence increase the current. The effect of secondary electrons emitted from the electrode by the bombardment of ions can also contribute to the increase in net current. Shamim *et al* [8] has measured the effect of electron emission from the electrode for high negative biases and has shown that the current from the secondary electron emission can be significant.

In the falling part of the pulse ($6{\cdot}0$ to $12{\cdot}0\,\mu$s) the experimental current becomes negative and then goes to zero. A negative electrode current during the pulse is observed earlier [1]. The model does not predict the negative current rather the current predicted by the model goes on decreasing from its value at $6{\cdot}0\,\mu$s. The discrepancy during this period can be explained qualitatively as the effect of reduction of the net charge inside the sheath with time. This is happening because the sheath is contracting due to the effect of reduction of the bias. As $(\mathrm{d}Q/\mathrm{d}t)$ is negative, where Q is the charge, the current driven is negative. To quantify this effect one must have the idea of the sheath capacitance. Even during the rise time of the pulse as $(\mathrm{d}Q/\mathrm{d}t)$ is positive, a positive current can be driven. The details of this technique and its feasibility are discussed later. In a recent paper Wood *et al* [17] have shown that when the decay period of the pulse is much slower the current does not go negative. In the experiments performed by us and ref. [1] the decay period is much faster to bring the effect of $(\mathrm{d}Q/\mathrm{d}t)$.

In § 3·1 it is stated that the present collisional sheath model is valid for α ranging between 0·2 and 1·0. At this point we would like to discuss the experiments already carried out [1–3]. Though the approach used there is much similar to ours, i.e., equating the current demanded by the collisional sheath to the current generated by the sheath expansion, the value of $\alpha \ll 0{\cdot}2$. Hence their experiment is carried out in an intermediate range of degree of collisionality, and the sheath cannot be treated as either fully collisionless or fully collisional.

The validity of the limit on α is also checked in the present study. By keeping all the experimental conditions same but by lowering the pressure (10^{-4} torr) the electrode current is measured during the application of the pulse. Though the mean

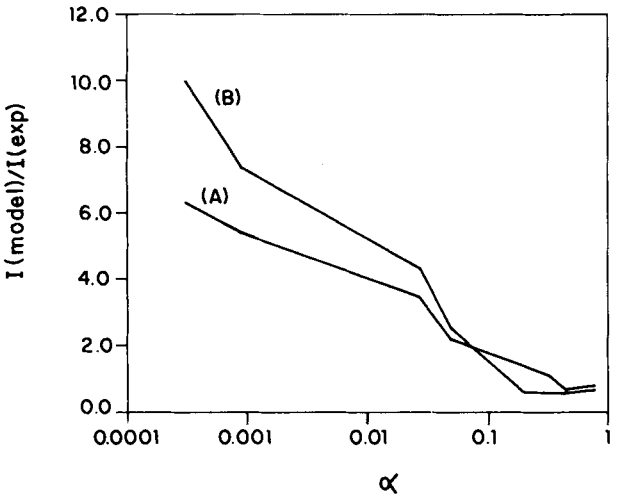

Figure 7. I(model)/I(exp) vs. α at (A) $t = 1{\cdot}4\,\mu$s and (B) $t = 3{\cdot}7\,\mu$s. The value I(model)/I(exp) is approaching unity for $\alpha > 0{\cdot}2$, indicating the validity of eqs (17), (20) and (23) for this degree of collisionality.

free paths are much larger than λ_d at this pressures still eqs (17), (20) and (23) are used to calculate the current. The previous calculations indicate that eqs (17), (20) and (23) are valid for $0{\cdot}2 < \alpha < 1{\cdot}0$. So for $\alpha < 0{\cdot}2$, the following equations is not a right description of the sheath dynamics. For lower pressures (10^{-4} torr), $\alpha \ll 0{\cdot}2$, the above equations are still used so as to indicate the range of applicability of the entire approach. At a given time, the ratio of the current predicted by the model (I_{model}) and measured current (I_{exp}) for various α is plotted in figure 7. Figure 7 indicates, that for small values of α the model is not a good description of sheath dynamics because the model predicts a current much larger than that measured in the experiment. But for $\alpha \geqslant 0{\cdot}2$, the agreement between the model and the experiment is good. Ideally for $\alpha \geqslant 0{\cdot}2$, ($I_{\text{model}}/I_{\text{exp}}$) should be unity. But it is less than unity because of the discrepancies already discussed earlier. Hence the limit on α discussed in § 3·1 is valid.

In the modeling of plasma source ion implantation and collisionless ion sheath dynamics, Wood [10] has proposed an alternate current calculation technique. The same technique can be extended for collisional ion sheath dynamics for better agreement in the experimental and model currents. The dynamic sheath plasma interface, which is at plasma potential, and the biased electrode can act as the two electrodes of a capacitor. As the interface moves in the plasma because of the current requirements of the target the entire phenomenon can be viewed as a change in net charge content in the sheath. Hence,

$$I = \mathrm{d}Q/\mathrm{d}t = C\mathrm{d}V/\mathrm{d}t + V\mathrm{d}C/\mathrm{d}t. \tag{24}$$

When the flow of ions is planar and satisfy Child's law (eq. 9) Bull [18] has shown that $C \approx 2\varepsilon_0 \times (\text{area})/x$, where x is the distance between the electrode and the sheath plasma interface and area denotes the area of the electrode. For a collisional ion sheath the value of sheath capacitance is yet to be found out.

Equation (24) thus gives the current for the dynamic sheath and it is possible to

give a qualitative picture of the sheath dynamics at each phase of the pulse. During the rise time (dV/dt) is positive but (dC/dt) is negative as the sheath thickness is increasing. A competition between (CdV/dt) and (VdC/dt) exists, but as C is a secondary effect of sheath expansion, (VdC/dt) will be less than (CdV/dt) and the current will increase. In the flat top phase of the pulse (dV/dt) is zero, but the sheath expands and hence the current reduces from its value at the end of the rise time of the pulse, and this can be given by (VdC/dt). In the decay phase of the pulse, (CdV/dt) is now negative but (VdC/dt) is positive. As (dV/dt) is larger during the initial part of the decay phase the current is driven negative from where it goes to zero as all time derivatives vanish. The difficulty in this entire technique is a right estimation of the dynamic capacitance when the sheath is collisional. Our ignorance of the value of the capacitance makes us unable to use this technique.

5. Conclusion

An experiment is performed by giving a pulsed negative bias on a disc electrode immersed in a collisional plasma. The pulse is characterized by a linear rise time followed by a flat top phase and then an exponential decay. A collisional sheath model is developed using the fluid equations and the limits on the degree of collisionality are found when this model is valid.

The model is further extended to study the dynamic evolution of a collisional ion sheath using the actual pulse shapes of the experiment. The effort is to explain the entire current profile. A good agreement is seen between the measured and the model current during the rise time and flat top phase of the pulse. In the falling part of the pulse the agreement is not satisfactory because of the exclusion of the role played by the negative rate of change of net charge in the sheath (dQ/dt). The residual discrepancies can be due to expansion of the sheath in other dimensions, secondary electron emission from the electrode by ion bombardment. An alternate current calculation scheme based on the concept of an expanding capacitor is also discussed. Presently efforts are made to estimate the value of the capacitance in the collisional ion sheath so that the alternate current calculation scheme can be implemented.

It is necessary to have a brief discussion regarding the merits and shortcomings of the model. Firstly the model is valid for a very small range of α, from 0·2 to 1·0, as indicated in figure 4. It cannot be extrapolated to lower values of α, because the convective term (uu') begins to give its contribution in the ion momentum equation. This model is valid for one dimensional planar sheath expansion and that too without the contribution of the secondary emitted electrons. In an experiment the sheath expands in all the directions and secondary electrons are also emitted, and both the processes enhances the current. In spite of its shortcomings and restricted region of application, the model has one merit, it is closer to the measured current by a factor less than 10%. This is of great help is plasma processing, where a prior knowledge of the electrode current and the corresponding sheath dynamics, helps in designing the power supplies, in deciding the spacing between target electrodes, etc.

Acknowledgements

The authors would like to thank Prof. A Sen, Dr H Ramchandran and Dr R Singh for useful discussions and suggestions.

References

[1] S Qin, C Chan, N E McGruer, J Browning and K Warner, *IEEE Trans. Plasma Sci.* **19**, 1272 (1991)
[2] S Qin and C Chan, *IEEE Trans. Plasma Sci.* **20**, 569 (1992)
[3] S Qin, C Chan, J Browning and S Meassick, *J Appl. Phys.* **74**, 1548 (1993)
[4] J R Conrad, R A Dodd, F J Worzala and X Qiu, *Surface and Coatings Technology* **36**, 927 (1988)
[5] M Shamim, J T Scheuer and J R Conrad, *J. Appl. Phys.* **69**, 2904 (1991)
[6] S M Malik, R P Fetherson, K Sridharan and J R Conrad, *Plasma Sources Sci. Technol.* **2**, 81 (1983)
[7] J T Scheuer, M Shamim and J R Conrad, *J. Appl. Phys.* **67**, 1241 (1990)
[8] M M Shamim, J T Scheuer, R P Fetherson and J R Conrad, *J. Appl. Phys.* **70**, 4756 (1991)
[9] R A Stewart and M A Liberman, *J. Appl. Phys.* **70**, 3481 (1991)
[10] B P Wood, *J. Appl. Phys.* **73**, 4770 (1993)
[11] M A Liberman, *J. Appl. Phys.* **65**, 4186 (1989)
[12] F B A Frungel, in *High Speed Pulse Technology* edited by F B A Frungel (Academic Press, New York, 1965) Vol. 1, p. 234
[13] T E Sheridan and J Goree, *Phys. Fluids* **B3**, 2796 (1991)
[14] F F Chen, in *Introduction to Plasma Physics* edited by F F Chen (Plenum, New York, 1974) p. 248
[15] T E Sheridan and J A Goree, *IEEE Trans. Plasma Sci.* **17**, 884 (1989)
[16] V Vahedi, M A Liberman, M V Alves, J P Verboncoeur and C K Birdsall, *J. Appl. Phys.* **69**, 2008, (1991)
[17] B P Wood, I Hennins, R J Gribble, W A Reass, R J Faehl, M A Nastasi and D J Rej, *J. Vac. Sci. Technol.* **B12**, 870 (1994)
[18] C S Bull, *Proceedings of the Institution of Electrical Engineers* **B104**, 374 (1957)